COMMUNICATION

Blue fluorescent dihydro-indenoindene derivatives with unusual low oxidation potentials as multifunctional OLED materials†

Yi Wei,*[a] Wei-Jyun Wang,[a] Yu-Ting Huang,[a] Bo-Cheng Wang,[a] Wen-Hao Chen,[a] Sang-Hsiu Wu[a] and Chiu-Hui He[b]

Several stable, blue fluorescent bis(diarylamino)dihydro-indenoindene derivatives were synthesized and used as materials for organic light-emitting diodes (OLEDs). The obtained HOMO energies reached up to 4.79 eV and under an applied voltage of 11 V, the current density generated by the hole only devices was 1161 mA cm^{-2}, showing their excellent hole mobility.

In the past few decades, aromatic compounds have been widely investigated for their potential in non-linear optics,[1] optical switches,[2] data storage,[3] chemical and biological sensing,[4] flat-panel displays,[5] and sustainable energy.[6] Some of these discoveries have eventually become commercial and enhance our everyday lives. Organic light-emitting diodes (OLEDs), which are one of the most innovative technologies for high-resolution displays and lighting,[7] are basically composed of electrodes, charge transporting layers, and high emissive R–Y–G–B layers. Notably, molecular architecture plays a dominant role in the design of these materials. While regarding the candidates, bis(diarylamino)dihydro-indenoindene derivatives (Scheme 1) that integrate two diarylamino units at the 2- and
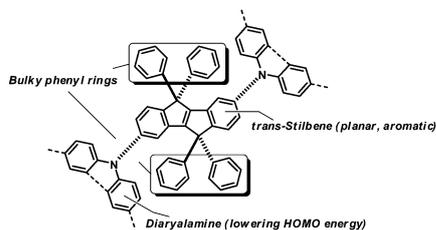
**Scheme 1** Concept of designing fluorescent dihydro-indenoindene derivatives.

[a]*Department of Chemistry, Tamkang University, No. 151, Yingzhuan Rd., New Taipei City 25137, Taiwan, Republic of China. E-mail: ywei@mail.tku.edu.tw*

[b]*Department of Chemistry, National Taiwan Normal University, No. 88, Sec. 4, Tingchow Rd., Taipei City, 11677, Taiwan, Republic of China*

7-positions of the 5,5,10,10-tetraphenyl-5,10-dihydro-[2,1,*a*]-indenoindene (**1**)[8] catch my eye because of their unique structures. The dihydro-indenoindene has 14 π electrons (aromatic) and because they are more delocalized than the anti-aromatic π electrons in dibenzopentalene (16 electrons), the additional electrons or holes generated at the opposite diarylamino substituents in this framework can communicate more easily. From another point of view, bis(diarylamino)stilbenes are well-known highly fluorescent molecules. **1** can be taken as a constrained *trans*-stilbene. This rigid structure prohibits the photo-isomerization process, therefore allowing us to utilize this highly emissive chromophore in OLEDs. The unfavorable non-radiative decay is also reduced because direct substitutions at the methylene carbons consolidate the molecule.

As illustrated in Scheme 2, the precursor **1** has been reported through multi-step synthesis.[8b,c] Unfortunately, the promising yield is not reproducible in our hands due to the lack of some essential apparatus. When we carried out the reactions reported in the literature, the conditions became more complicated owing to the incomplete air- and moisture-isolation in a simple Schlenk line. The large amount of byproducts produced caused difficulties in purification and resulted in the low yield in each step. We therefore established a new synthetic route deriving from the addition of a *cis*-stilbene moiety to benzophenone through a halogen–metal exchange reaction. The resulting tertiary alcohol was then dehydrated intramolecularly. According to our approach, it can be synthesized in 2 steps without crucial purifications,[9] and the overall yield is competitive to the original method (24% and 25%, respectively). Moreover, direct bromination of **1** successfully yields the other precursor **2**, on which the Buchwald–Hartwig coupling reactions were performed to obtain the target molecules **3a–c** in good yields. Based on the orientation in three dimensions, these molecules are highly symmetrical and nonpolar. However, we suppose the rigid structures inhibit the effective π–π stacking to any other aromatic compound. It makes them barely soluble in common organic solvents such as pyridine, benzene, and toluene. The fraction works were done by sublimation under reduced
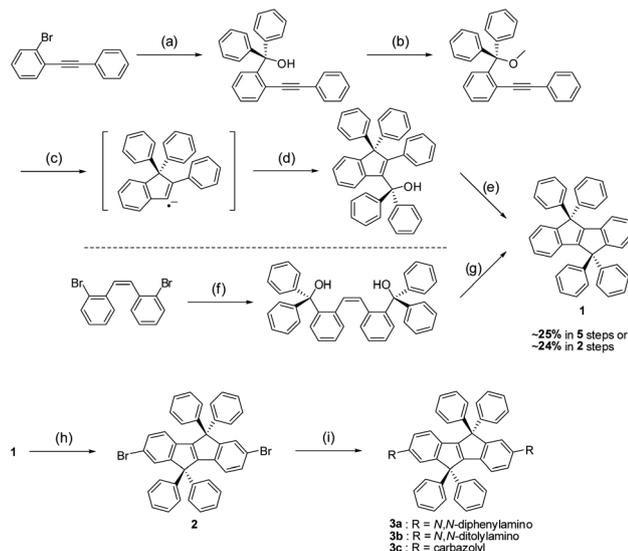
Scheme 2 Synthetic strategy for 1–3. Reagents and conditions: (a) *n*-BuLi and benzophenone, ether, 0 °C, 1 h. (b) CAN, MeOH, reflux, 16 h. (c) Li and naphthalene, THF, r.t., 30 min. (d) benzophenone, THF, r.t., 30 min. (e) BF₃·OEt₂, CH₂Cl₂, r.t., 1 h. (f) *n*-BuLi and benzophenone, ether, 0 °C, 2 h. (g) cat. HCl, acetic acid, reflux, 4 h. (h) CuBr₂/Al₂O₃, CCl₄, reflux, 30 h. (i) Pd₂(dba)₃, P(*t*-Bu)₃, NaO*t*-Bu, and the corresponding amine, toluene, reflux, 4 h.

Fig. 1 Diagram of HOMO (left) and LUMO (right) surfaces for **3a–c**.

pressure. All the molecular structures were identified by NMR spectroscopy.

The steady-state photophysical properties of **3a–c** in CH₂Cl₂ were identified at ambient temperature. As summarized in Table 1, the maximum absorption peaks (Abs. $\lambda_{\max}$) obtained are in the order of **3b** (427 nm) > **3a** (422 nm) > **3c** (385 nm), which is consistent with the DFT calculation results.[9] The calculated values for **3a–c** are 439, 446 and 410 nm, respectively. We conclude that this trend is attributed to the extent of the electron donating nature of different diarylamino substituents, and **3b** has a slight bathochromic shift in absorption compared to the others. On the other hand, all the longest absorptions for these molecules result in $S_0 \rightarrow S_1$ electronic transitions. Their molecular orbital surfaces show that the π electrons in the HOMOs are delocalized in the whole molecule except in the perpendicular phenyl rings. However, they are mainly localized in the central *trans*-stilbene fragment in the LUMOs (Fig. 1).

Upon excitation, **3a–c** emit sky blue fluorescence. The maximum emission peaks (Em. $\lambda_{\max}$) are observed at 452, 459, and 434 nm, with an individual full width at half maximum (fwhm) of 53 ± 6 nm. The narrow emission profiles, as well as
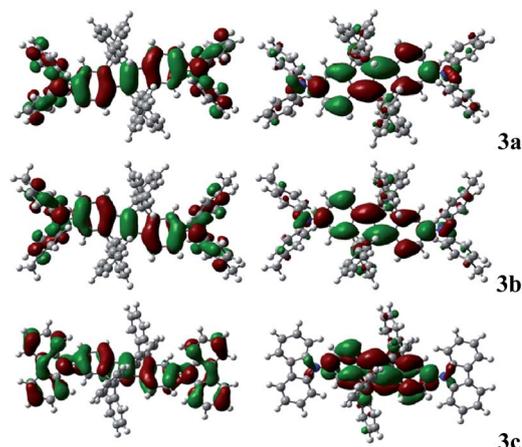
high external quantum yields (Φ_f) up to 80%, indicate that these molecules may be utilized as good emitting materials.

They also exhibit excellent thermal stability because of their rigid structures. The T_d values were recorded in the range of 492–546 °C, and the phenyl rings hanging at the 5- and 10-positions of the central dihydro-indenoindene framework may contribute to the high T_g (163–204 °C). In addition, the redox behaviours were evaluated by CV experiments using ferrocene as an internal reference.[10] The first oxidation potentials (E_{ox}) of **3a–c** which can be correlated to their HOMO energy levels were observed reversibly at +0.21, −0.01 and +0.69 V, respectively. Notably, owing to the pendent electron donating diarylamino units, **3a and b** have extremely high HOMO energies compared with **3c** (with carbazolyl units instead) and other organic compounds (Fig. 2). The difference in values ($\Delta E = 0.22$ V) between **3a and b** is attributed to the methyl substitution at the *para*-position of the anilyl group. A similar tendency can also be
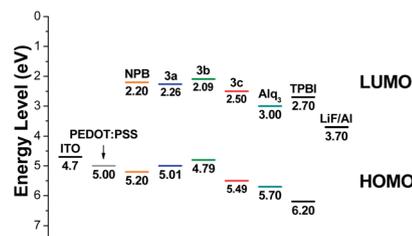

Fig. 2 Illustration of relative energy levels.

Table 1 Morphological, photophysical, and electrochemical data for **3a–c**

	Abs. $\lambda_{\max}^{a,b}$ (nm)	Abs. $\lambda_{\max}^{c,d}$ (nm)	Em. $\lambda_{\max}^{a,e}$ (nm)	Φ_f (%)	T_g/T_d (°C)	$E_{ox}{}^a$ (V)
3a	310 (20.4), 404 (38.0), 422 (35.5)	439 (0.909)	452 (51)	49	163/492	+0.21, +0.33
3b	310 (19.7), 410 (34.2), 427 (33.1)	446 (0.959)	459 (47)	47	165/514	−0.01, +0.21
3c	294 (26.9), 370 (37.7), 385 (31.6)	410 (0.674)	434 (59)	80	204/546	+0.69

a Measured in CH₂Cl₂. *b* The data in parentheses correspond to $\varepsilon \times 10^{-3}$. *c* Simulated by the DFT/TD-DFT model. *d* The data in parentheses are *f* (relevant to absorption intensities). *e* The data in parentheses correspond to fwhm.

1780 | *J. Mater. Chem. C*, 2014, **2**, 1779–1782

This journal is © The Royal Society of Chemistry 2014

Table 2 Summary of the EL results in OLED devices for **3a–c**

Device Config.[a]	Em. λ_{max}[b] (nm)	V_{on}[c] (nm)	η_c[c]/η_p[c] (cd A^{-1}/lm W^{-1})	L_{20}[c] (cd m^{-2})
3a/A	460, 484 (88)	2.5 (4.6)	2.8/1.9	551
3a/B	456, 484 (88)	2.5 (5.0)	2.4/1.5	476
3a/C	532 (107)	3.1 (7.9)	3.0/1.2	590
3b/A	468, 492 (82)	2.5 (4.8)	2.8/1.9	563
3b/B	464, 484 (70)	2.5 (4.5)	2.4/1.6	471
3b/D	468, 492 (83)	2.5 (5.2)	3.6/2.2	712
3c/A	432, 452 (76)	3.0 (4.7)	1.8/1.2	347
3c/B	432, 448 (76)	3.1 (5.6)	1.6/0.9	324
NPB/E	532 (100)	2.5 (4.1)	2.6/2.0	530

[a] Device configuration: A: ITO/**3a–c** (40 nm)/TPBI (40 nm)/LiF (1 nm)/Al; B: ITO/NPB (40 nm)/**3a–c** (40 nm)/TPBI (40 nm)/LiF (1 nm)/Al; C: ITO/**3a** (20 nm)/Alq$_3$ (40 nm)/LiF (1 nm)/Al; D: ITO/PEDOT:PSS (30 nm)/**3b** (40 nm)/TPBI (40 nm)/LiF (1 nm)/Al; E: ITO/NPB (40 nm)/Alq$_3$ (40 nm)/LiF (1 nm)/Al. [b] The data in parentheses correspond to fwhm. [c] η_c, η_p, L_{20}, and the data in parentheses of V_{on} were measured at 20 mA cm^{-2}.

observed in the increase of their LUMO energy levels. This unusual phenomenon may facilitate the hole injection from the cathode, and thus enhance the corresponding optoelectronic performances. We did a preliminary study of **3a**.[9] Under the same applied voltage of 11 V, the current density measured for the hole only device (ITO/NPB[11]/**3a**/NPB/LiF/Al) is 1161 mA cm^{-2}, which is ~480 times higher than the value (2.4 mA cm^{-2}) obtained from the electron only device (ITO/BCP/**3a**/TPBI[12]/LiF/Al). This dramatic difference suggests that these molecules may be adequate for hole transports. As others support, it is higher than the data reported for several known hole transporting (HT) materials (TCTA, *etc.*).[13]

In order to examine our assumptions, two types of OLEDs devices were made for advanced inspection. **3a–c** were utilized as both HT and emitting materials in combination with the commercial electron transporting (ET) material TPBI in the bilayer devices (configuration A). On the other hand, trilayer devices (configuration B) where **3a–c** only work as emitting materials can be fabricated by depositing a layer of NPB on the top of the cathode (indium tin oxide, ITO) due to its excellent hole mobility.[11] The EL data are summarized in Table 2. All these devices exhibit highly efficient sky-blue fluorescence. The emission profiles reveal a vibronic feature, showing two λ_{max} peaks in the range of 474 ± 18 and 442 ± 10 nm for **3a and b** and **3c**, respectively. In device-A, the low turn-on voltages (V_{on}) for **3a and b** imply that the hole injection from ITO proceeds smoothly, and is identical to our prediction. Moreover, the luminance and power efficiencies (η_c/η_p) measured at 20 mA cm^{-2} are 2.8/1.9, 2.8/1.9, and 1.8/1.2 cd A^{-1}/lm W^{-1}, respectively, for **3a–c**. These performances are slightly ahead of those the corresponding trilayer devices display, furthermore, the enhancement (110–130%) is proportional to the relative operational brightness (L_{20}) obtained at 20 mA cm^{-2} (347–563 to 324–476 cd m^{-2}, ~115% on average). A more imbalanced ratio between the holes and electrons may result from the existence of additional HT material, and cause the inefficient charge recombination. Based on the preliminary results, we further utilize **3a** (configuration C) and NPB (configuration E) as simple HT materials where Alq$_3$ was chosen as the ET and emitting material based on its HOMO and LUMO energy levels. In comparison, similar emission profiles obtained from both

devices show that the holes are properly transported and injected into the emitting layer, and the η_c (3.0 cd A^{-1}) and L_{20} (590 cd m^{-2}) show 10–15% enhancement in device-C. According to these observations, we now confirm that **3a–c** work well as HT materials. An attempt to optimize the EL efficiency of **3b** was carried out by fabricating a tetralayer device (configuration D) where 30 nm of PEDOS:PSS[14] was spin-coated. Interestingly, a significant enhancement up to 50% was observed when this individual hole injection layer further fixed the interface between ITO and **3b**. The resulting η_c and η_p are 3.6 and 2.2, respectively, with an L_{20} of 712 cd m^{-2}.

Conclusions

In conclusion, we have developed a new strategy for the synthesis and purification of stable bis(diarylamino)dihydro-indenoindene derivatives. Their HOMO energies are close to the work function of ITO, which enables facile hole injection and high hole mobility. In OLEDs, these molecules show high sky blue fluorescence and serve as good HT materials. The bifunctional feature exhibited by the device in this study is useful for the simplification of the complex fabrication process.

Acknowledgements

Notes and references

1 (*a*) J. A. Delaire and K. Nakatani, *Chem. Rev.*, 2000, **100**, 1817; (*b*) P. A. Franken, A. E. Hill, C. W. Peters and G. Weinreich, *Phys. Rev. Lett.*, 1961, **7**, 118; (*c*) D. R. Kanis, M. A. Ratner and T. J. Marks, *Chem. Rev.*, 1994, **94**, 195; (*d*) H. Lin, W. Lin, H. Bai, J. Chen, B. Jin and T. Luh, *Angew. Chem., Int. Ed.*, 2007, **46**, 897.

2 (*a*) B. L. Feringa, R. A. van Delden, N. Koumura and E. M. Geertsema, *Chem. Rev.*, 2000, **100**, 1789; (*b*) B. L. Feringa, *Molecular Switches*, Wiley-VCH Verlag GmbH, 2001; (*c*) M. Irie, *Chem. Rev.*, 2000, **100**, 1685.

This journal is © The Royal Society of Chemistry 2014

J. Mater. Chem. C, 2014, **2**, 1779–1782 | **1781**

3 (*a*) L. Mayer, *J. Appl. Phys.*, 1958, **29**, 1003; (*b*) S. Ovshinsky, *US Pat.*, 3,530,441, 1970.

4 (*a*) L. Fan, Y. Zhang, C. B. Murphy, S. E. Angell, M. F. Parker, B. R. Flynn and W. E. Jones Jr, *Coord. Chem. Rev.*, 2009, **253**, 410; (*b*) J. S. Kim and D. T. Quang, *Chem. Rev.*, 2007, **107**, 3780; (*c*) R. Martínez-Máñez and F. Sancenón, *Chem. Rev.*, 2003, **103**, 4419; (*d*) D. T. McQuade, A. E. Pullen and T. M. Swager, *Chem. Rev.*, 2000, **100**, 2537; (*e*) S. W. Thomas, G. D. Joly and T. M. Swager, *Chem. Rev.*, 2007, **107**, 1339.

5 (*a*) K. Müllen and U. Scherf, *Organic Light-Emitting Devices. Synthesis, Properties and Applications*, Wiley-VCH Verlag GmbH & Co. KGaA, 2005; (*b*) C.-H. Chen and S.-W. Huang, *OLED/Organic Electroluminescent Materials & Devices*, Wunan Press, 2005; (*c*) M.-B. Tien and Y.-H. Lin, *Principles and Technologies of Liquid Crystal Displays*, Wunan Press, Taipei, Taiwan, 2008; (*d*) J. H. Burroughes, D. D. C. Bradley, A. R. Brown, R. N. Marks, K. Mackay, R. H. Friend, P. L. Burns and A. B. Holmes, *Nature*, 1990, **347**, 539.

6 (*a*) B. O'Reagen and M. Grätzel, *Nature*, 1991, **353**, 737; (*b*) A. Yella, H. Lee, H. N. Tsao, C. Yi, A. K. Chandiran, M. K. Nazeeruddin, E. W. Diau, C. Yeh, S. M. Zakeeruddin and M. Grätzel, *Science*, 2011, **334**, 629; (*c*) C.-C. M. Ma, *Organic Solar Cells and Plastics Solar Cells*, Wunan Press,

2008; (*d*) P. C. Ewbank, D. Laird and R. D. McCullough, *Organic Photovoltaics*, Wiley-VCH Verlag GmbH & Co. KGaA, 2009.

7 C.-H. Chen, C.-T. Chen and C.-C. Wu, *White OLED Lighting*, Wunan Press, 2009.

8 (*a*) X. Zhu, C. Mitsui, H. Tsuji and E. Nakamura, *J. Am. Chem. Soc.*, 2009, **131**, 13596; (*b*) X. Zhu, H. Tsuji, K. Nakabayashi, S. Ohkoshi and E. Nakamura, *J. Am. Chem. Soc.*, 2011, **133**, 16342; (*c*) D. Hellwinkel, H.-J. Hasselbach and F. Lammerzahl, *Angew. Chem., Int. Ed*, 1984, **23**, 705.

9 See ESI† for the complete syntheses of **1**–**3**, computational data for **3a**–**c**, and device details for **3a**–**c**, and NPB.

10 G. Gritzner and J. Kuta, *Pure Appl. Chem.*, 1984, **56**, 461.

11 (*a*) B. E. oene, D. E. Loy and M. E. Thompson, *Chem. Mater.*, 1998, **10**, 2235; (*b*) D. F. O'Brien, P. E. Burrows, S. R. Forrest, B. E. Koene, D. E. Loy and M. E. Thompson, *Adv. Mater.*, 1998, **10**, 1108.

12 J. Shi, C. W. Tang and C. H. Chen, *US Pat.*, 5,645,948, 1997.

13 (*a*) W. Zhang, Z. Wu, X. Zhang, S. Liang, B. Jiao and X. Hou, *Chin. Sci. Bull.*, 2011, **56**, 2210; (*b*) T. Hirai, K. Weber, J. O'Connell, M. Bown and K. Ueno, *Jpn. J. Appl. Phys.*, 2013, **52**, 04CK02.

14 A. Elschner, F. Bruder, H. Heuer, F. Jonas, A. Karbach, S. Kirchmeyer, S. Thurm and R. Wehrmann, *Synth. Met.*, 2000, **111**, 139.